J. Plasma Physics (2005), *vol.* 71, *part* 6, *pp.* 859–875. © 2005 Cambridge University Press
doi:10.1017/S0022377805003697 Printed in the United Kingdom

Quasi steady-state distributions for particles with power-law interaction potentials

I. F. POTAPENKO[1], M. BORNATICI[2] and V. I. KARAS[3]

[1]Keldysh Institute for Applied Mathematics, RAS, 125047 Moscow, Russian Federation
[2]Department of Physics "A. Volta", University of Pavia, I 27100 Pavia, Italy
[3]Kharkov Institute of Physics and Technology, UAS, 310108 Kharkov, Ukraine
(firena@yandex.ru)

(Received 6 September 2004)

Abstract. The formation of a non-equilibrium steady-state distribution function of particles with the power law interaction potentials $U = \alpha/r^{s}$, where $1 \leqslant \beta < 4$, is studied numerically. Consideration is based on the one-dimensional nonlinear kinetic equation of a Landau–Fokker–Planck type in the presence of particle (energy) sources. Non-equilibrium quasi steady-state local distributions exist inside the momentum interval between the energy (particle) source and the bulk (or sink) of the particle distribution and have the form of gradually decreasing functions. Numerical calculations based on the completely conservative difference schemes are accompanied by the analytical consideration and comparison with the experimental results is given. Obtained results can be useful in connection with the development of high-power particle and energy sources and for the prediction of the semiconductors behavior with an intrinsic or extrinsic conductivity under the action of particle fluxes or electromagnetic radiation.

1. Introduction and statement of the problem

Non-ideal plasma systems where the evolution of the distribution in the presence of a particle (energy) source involves the effect of externally imposed waves (quasilinear flattening), have been the subject of different studies in the non-equilibrium (NE) states of various physical systems. The analysis of the NE distributions attract increasing interest, particularly in connection with the development and wide use of high-power particle and energy sources. In the theory of turbulence of incompressible liquids, a universal (independent of the structures of the source and sink) steady-state NE energy spectrum in the wave number range between the wave numbers of the excited and efficiently damped motions, was first obtained in [1]. In the theory of weak turbulence, universal wave spectra in the form of solutions to equations with the wave–wave collision integral were derived in [2]. Steady-state NE power-like particle distributions, being the exact solutions of the Boltzmann collision kinetic equation in the presence of particle (energy) sources and sinks in momentum space, were obtained in [3]. The anomalously high photoconductivity of a semiconductor irradiated by light, which frequency is insufficient to cause an interband transition, may be explained by the formation of a NE distribution of electrons and holes. It was experimentally shown that the irradiation of semiconductors by α-particles may substantially change their conduction properties. Some

https://doi.org/10.1017/S0022377805003697 Published online by Cambridge University Press

experimental data on the emission current from metals irradiated by lasers can be reasonably explained by the mechanism for the formation of NE distributions [4–8]. It was shown [3,6,8] that, for a semiconductor plasma in the energy range $E-E_{\rm F} > E_{\rm F}$ (where $E_{\rm F}$ is the Fermi energy) a power-like distribution with a non-zero flux of energy or particles in momentum space can be established. This NE distribution function is formed both due to collisions with electrons whose energy is in the range $E-E_{\rm F} > E_{\rm F}$ and background (equilibrium) electrons. For the existence of such local stationary NE solutions, it is necessary to satisfy many rigorous conditions that in real physical systems are difficult to fulfil. The analytical consideration of the NE distribution function formation in the case of non-stationary, non-localized, mismatched on intensity sources and sinks is very problematic, thus numerical treatment must be used. For the numerical investigation of the problem, we develop the original conservative schemes whose efficiency is proved in different problems (see, for instance, [8, 9]).

In our opinion, the formation of NE distributions in the presence of external pumping and the physical effect associated with such fundamental changes in the electron distribution function is an interesting problem that is discussed in the present paper. We analyze the formation of steady-state NE distributions for spatially homogeneous isotropic plasma consisting of electrons with sources (sinks) localized in a momentum space. The energy (particle) source and sink can be provided by ion beams, high-power laser radiation, emission currents, and fluxes of charged particles produced in fusion or fission reactions. The treatment is based on the Landau–Fokker–Planck (LFP)-type equation, which is a model of Boltzmann's equation for arbitrary interaction potentials [10, 11], and briefly considered below. It is worth mentioning that obtaining the rigorous mathematical results is quite uncertain even for the linearized LFP equation. Starting from the one-dimensional LFP-type equation in the presence of weak sources, we study the asymptotic solutions in the high-energy region for power-like interaction potentials $U \sim \alpha/r^{\beta}$, $1 \leqslant \beta < 4$ in Sec. 2. In Sec. 3 we study the temporal evolution of the NE function numerically and analyze the structure of the steady-state distribution functions and its dependence on different parameters (intensities, source locations, exponents in the interaction potential, etc.) in detail. Asymptotic results are confirmed by numerical calculations with high accuracy and the comparison of the numerical calculations with the analytical asymptotic results, in turn, proves the high accuracy of the exploited difference schemes. On the basis of fulfilled study the satisfactory analysis of the concrete experimental situation [8] is performed and a qualitative comparison with results from [7] is given. Conclusive remarks are given in Sec. 4.

In this paper we use the model of Boltzmann's equation for the distribution function $f(\mathbf{v}, t)$:

$$\frac{\partial f}{\partial t} = \hat{J}[f, f] = \int d\mathbf{w}\, d\mu\, d\phi\, u\sigma(u, \mu)[f(\mathbf{v}')f(\mathbf{w}') - f(\mathbf{v})f(\mathbf{w})], \quad t \geqslant 0, \qquad (1)$$

which approximates the integral operator $\hat{J}[f, f]$ (1) for arbitrary potentials by an integro-differential operator of LFP type. Note that in Boltzmann's equation, the only quantity depending on the molecular interaction law is the differential cross section $\sigma(u, \cos\theta)$, where $u > 0$ is the relative speed. The construction of the cross section $\sigma(u, \mu)$ with the given interaction potential $U(r)$ is a well-known problem of classical mechanics [12, 13]. We compare the real gas of particles with its analogue

https://doi.org/10.1017/S0022377805003697 Published online by Cambridge University Press

having another cross section: $\tilde{\sigma}(u, \cos\theta) = 0$ for $\theta > \theta_0$, where $\theta_0 \ll 1$ is the scattering at small angles. Hence, in the model Boltzmann equation, the exact collision integral can be replaced by the approximation $\hat{J}[f, f] \approx \hat{I}[f, f][1 + O(\theta_0)]$, as $\theta_0 \to 0$. For real intermolecular potentials, the contributions from scattering at large and small angles have approximately the same order of magnitude. Nevertheless, the last approximation could be used for arbitrary cross sections if the fundamental criterion of the chosen approximation in the proposed model is the number of identical moments of the exact and the approximate collision integrals. Then, the problem consists of an adjustment of the new scattering cross section $\tilde{\sigma}(u, \mu)$ in order to achieve the coincidence of the macroscopic characteristics of the original with that of the model gases:

$$\int d\mathbf{v}\, \phi(\mathbf{v}) \hat{J}[f, f] = \int d\mathbf{v}\, \phi(\mathbf{v}) \hat{I}[f, f], \tag{2}$$

where $\phi(\mathbf{v})$ is an arbitrary function. When this problem is solved, then instead of Boltzmann's integral equation (1), the simplified collision integral of LFP type can be considered:

$$\frac{\partial f}{\partial t} = \hat{I}[f, f] = \frac{1}{8} \frac{\partial}{\partial v_i} \left\{ \int d\mathbf{w}\, u\sigma(u)(u^2 \delta_{ij} - u_i u_j) \left(\frac{\partial}{\partial v_j} - \frac{\partial}{\partial w_j} \right) f(\mathbf{v}) f(\mathbf{w}) \right\}. \tag{3}$$

Here

$$\sigma(u) = \int d\mu\, d\phi\, \tilde{\sigma}(u, \mu)(1 - \mu) = \tfrac{1}{2} \int d\mu\, d\phi\, \sigma(u, \mu)(1 - \mu^2). \tag{4}$$

The moments of the exact collision integral $\hat{J}[f, f]$ (1) with its model $\hat{I}[f, f]$ (3) coincide up to the tensor third-order moment as well as up to the fourth-order scalar moment irrespectively of the interaction potential form. That is, the equality (2) is valid for the functions $\phi(\mathbf{v}) = \{v_i v_k,\ v_i v_k v_l,\ i, k, l = 1, 2, 3; v^4\}$. The same conservation laws of the particle density, the moment and the energy as well as the Boltzmann H-theorem are valid for the model (3). It leads to the correct moment equations up to Grad's 20th-moment approximation [12]. By inserting the 'cut-off' Rutherford cross section $\sigma(u, \theta) = (e^2/mu^2)^2 \sin^{-4}(\theta/2) \eta[\theta - \theta_{\min}]$ into (4) we get $\sigma(u) \approx 8\pi(2e^2/mu^2)^2 L$ where $L = \ln \theta_{\min}^{-1}$, as $\theta_{\min} \to 0$, and one can obtain the well-known classical LFP equation for plasmas [14, 15]. Finally, for the so-called Maxwell's molecules, $U \sim \alpha/r^4$ [12], the exact solution of the approximate equation (3) is the solution of the exact Boltzmann equation (1) [16].

The points enumerated above are on the credit side for the considered model. However, a LFP-type equation contains an operator of diffusion type, which leads to instantaneous smoothing of discontinuities in the initial conditions, and for Boltzmann's operator with a short-range intermolecular potential such discontinuities are preserved, since there is some number of particles not experiencing collisions for any finite interval. This distinction emphasizes that the natural sphere for the application of the model (3) are gases with potentials of an infinite radius of action, $U \sim \alpha/r^\beta$, $1 \leqslant \beta < 4$, because for these potentials Boltzmann's equation itself must also possess smoothing properties. Note that $\beta = 1$ corresponds to the Coulomb interaction of charged particles, $\beta = 2$ corresponds to the dipole interaction, and $\beta = 4$ corresponds to the so-called Maxwellian molecules.

https://doi.org/10.1017/S0022377805003697 Published online by Cambridge University Press

2. LFP-type equation with weak sources located in the high-velocity region

To reveal the principal aspects of the problem under consideration, we begin with the asymptotic approach and first present the analytical solution in the linear case, which is correct for the high-velocity region, and give the rigorous asymptotic conditions of the solution validity.

For the isotropic distribution function, the collision integral (3) can be written as

$$\hat{I}[f,f]=\frac{1}{v^2}\frac{\partial}{\partial v}\left\{\frac{1}{v}\int_0^\infty dw\,Q(v,w)\left[wf(w)\frac{\partial f(v)}{\partial v}-vf(v)\frac{\partial f(w)}{\partial w}\right]\right\}, \tag{5}$$

where the symmetric kernel $Q(v,w)$ is

$$Q(v,w)=\frac{\pi}{8}v^3w^3\int_{-1}^{1}d\mu(1-\mu^2)u\sigma(u),\quad u^2=v^2+w^2-2vw\mu.$$

Our consideration is based on the kinetic equation that includes external sources (sinks) of energy (particles):

$$\frac{\partial f(v,t)}{\partial t}=\hat{I}[f,f]+\frac{n_{\mathrm{S}}}{t_{\mathrm{S}}}S(v),\quad f|_{t=0}=f_0(v);\quad 0\leqslant v<\infty,\ t\geqslant 0. \tag{6}$$

The particle density n and temperature T (average energy) expressed in energetic units are defined through integrals

$$n=(f,1)=4\pi\int_0^\infty dv\,v^2f(v,t),\quad T=\frac{m}{3n}(f,v^2)=\frac{4\pi m}{3n}\int_0^\infty dv\,v^4f(v,t),\quad t\geqslant 0, \tag{7}$$

where m is the electron mass. Without the source (sink) action, $S(v)=0$, the above equations should be completed by the conservation laws $n=n_0=$ constant and $T=T_0=$ constant. In this case the unique equilibrium solution of the problem is the Maxwellian distribution. It is worth mentioning that some power-like functions $f=C_1|v|^{p(\beta)}$, which match the interaction potentials $U=C_2r^{-\beta}$, turn the LFP-type collision integral to zero, and the Boltzmann operator can also be easily checked by the formal substitution. For Coulomb collisions these functions with $p(1)=-\frac{5}{2}$ correspond to the infinite energy in a full velocity space. We assume that the distribution function $f(v,t)$ is finite at $v=0$ and decreases fairly rapidly as $v\to\infty$ to provide the boundedness of integrals (7).

In general case, the source (sink) may depend on time, distribution function, etc. We restrict ourselves to the time independent sources with small intensities $n_{\mathrm{S}}/t_{\mathrm{S}}=\varepsilon\ll 1$. Then we go to the new time variable t/ε and obtain $\partial f/\partial t=\hat{I}[f,f]\varepsilon^{-1}+S$ for (6). Note that,

$$\frac{dn}{dt}=(S,1),\quad \frac{d}{dt}\left(\frac{3nT}{m}\right)=(S,v^2). \tag{8}$$

The formal solution of the former equation can be constructed in the frame of the Chapman–Enskog method in the form of a set $f=f_0+\varepsilon f_1+\cdots$. Then

$$f_0=f_{\mathrm{MW}}(t)=n\left(\frac{m}{2\pi T}\right)^{3/2}\exp\left(-\frac{mv^2}{2T}\right),$$

https://doi.org/10.1017/S0022377805003697 Published online by Cambridge University Press

where the time dependence of n, T is given by (8). As usual, the orthogonal conditions

$$(f_i, 1) = (f_i, v^2) = 0, \quad i = 1, 2, \ldots$$

are assumed. In new units the typical time of Coulomb collisions t_C is of order ε and the typical time of density and temperature alteration is of order 1. From this it is clear that, the intermediate regime $\varepsilon \ll t \ll 1$ might exist, when the relaxation chiefly is terminated but the density and the temperature still remain almost unvarying. We are now concerned with this intermediate asymptotic, although our conclusions are valid for $t \geqslant 1$, as well. We study a solution $f = f_0 + \varepsilon f_1$ in the limiting case, as $\varepsilon \to 0$. Function f_1 can be constructed as a solution to the non-uniform linearized equation

$$\partial f_0/\partial t = \hat{I}[f_0, f_1] + \hat{I}[f_1, f_0] + S$$

and the orthogonal conditions provide the solution uniqueness similarly, all f_i, for $i = 2, 3, \ldots$ can be defined. It should be noted that the Chapman–Enskog procedure, generally speaking, becomes incorrect in the vicinity of the source location where its influence cannot be considered as small. Therefore, it is unclear how many terms it is necessary to take in a sequence of f_i to obtain the main asymptotic term under condition $\varepsilon \ll 1$. To obtain a rigorous result, we turn the consideration of the linearized LFP equation to the linear case assuming sources located in a high-velocity region $v_{\text{th}} = \sqrt{T/m}$.

In the high-velocity region where the problem is substantially simplified, the collision LFP integral for any distribution function is transformed into

$$\hat{I}[f, f] = \frac{n}{8}\frac{1}{v^2}\frac{\partial}{\partial v}\left[v^3\sigma(v)\left(\frac{T}{m}\frac{\partial f}{\partial v} + vf\right)\right].$$

Here we take into account the fact that, in the high-velocity region the kernel $Q(v, w)$ reduces to $Q(v, w) \to \pi w^3 v^4 \sigma(v)/6$, as $v \to \infty$. Furthermore, for the power-law potentials, we employ the cross section $\sigma(u, \mu) = g_\beta(\mu) \cdot u^{-4/\beta}$ (see [10, 11]). By inserting this expression in (5), as $v \to \infty$, we obtain the equation

$$\frac{\partial f}{\partial t} = \frac{n g_\beta}{8}\frac{1}{v^2}\frac{\partial}{\partial v}\left[v^{3-4/\beta}\left(\frac{T}{m}\frac{\partial f}{\partial v} + vf\right)\right] + S, \tag{9}$$

where the notation

$$g_\beta = 2\pi \int_{-1}^{1} d\mu \, g_\beta(\mu)(1 - \mu^2) \tag{10}$$

is used. For instance, for the Coulomb potential with $\beta = 1$ formula (10) yields $g_1 = 32\pi e^4 L/m^2$, then the well-known linear LFP equation for plasmas follows from (9).

Then, we introduce scaled variables:

$$\tilde{v} = v/v_{\text{th}}; \quad \tilde{t} = t/t_\beta, \quad t_\beta = \frac{32\pi v_{\text{th}}^3}{n g_\beta} \cdot v_{\text{th}}^{4(\beta-1)/\beta}; \quad \tilde{f} = \frac{4\pi v_{\text{th}}^3 f}{n}, \quad \tilde{S} = \frac{4\pi v_{\text{th}}^3 t_S S}{n_S}.$$

Omitting tildes after the normalization and passing to the variable $x = v^2$, we write the LFP equation in a form:

$$\frac{\partial f(x,t)}{\partial t} = \frac{N}{x^{1/2}}\frac{\partial}{\partial x}\left\{x^\gamma\left[2\theta\frac{\partial f}{\partial x} + f(x)\right]\right\} + \varepsilon \cdot \frac{S(x)}{x^{1/2}}, \quad \gamma = 2\frac{\beta - 1}{\beta}, \quad \varepsilon = \frac{n_S t_C}{n_0 t_S}. \tag{11}$$

https://doi.org/10.1017/S0022377805003697 Published online by Cambridge University Press

Here N and θ represent the dimensionless density and temperature:

$$N = \int_0^\infty f x^{1/2}\, dx, \quad \theta = \frac{1}{3N}\int_0^\infty f x^{3/2}\, dx; \quad N_0 = \theta_0 = 1. \tag{12}$$

The parameter $\gamma = 0, 1$ and $\frac{3}{2}$ corresponds to the Coulomb, dipole interaction and Maxwell molecules, respectively.

Now we let $t = \tau/\varepsilon$ and, substituting f in (11) with $\varepsilon F(x)/N$, we obtain (as $\varepsilon \to 0$), the stationary equation

$$\frac{\partial}{\partial x}\left[x^\gamma\left(2\theta\frac{\partial F}{\partial x} + F\right)\right] + S(x) = 0, \tag{13}$$

which includes the time variable τ as a parameter (the argument of the functions N_τ, θ_τ defined by the (8), (12)). The question is how to choose correctly the partial solution that gives a solution of our problem under $x \gg 1$.

It is useful to represent the Maxwellian distribution $F_{\mathrm{MW}}(x)$ as follows:

$$\begin{aligned} F_{\mathrm{MW}}(x) &= \sqrt{\frac{2}{\pi}} N\theta^{-3/2} \exp\left\{-\frac{x}{2\theta}\right\} \\ &= \varepsilon\sqrt{\frac{2}{\pi}} N\theta^{-3/2} \exp\left\{-\left[\frac{x}{2\theta} - \ln\frac{1}{\varepsilon}\right]\right\} \\ &\equiv \varepsilon C \exp\{-y\}, \end{aligned} \tag{14}$$

where $y = x/2\theta - \ln 1/\varepsilon$. Seeking the unique solution to (13) we now additionally assume that the source $S(x - x_1)$ is localized at the point

$$x_1 = 2\theta_0\left(\ln\frac{1}{\varepsilon} + y_1\right), \tag{15}$$

where y_1 is a number, positive or negative, independent of ε. The source $S(x)$ is supposed to be a finite function which is normalized such that

$$\int_{-\infty}^{\infty} dx\, S(x) = 1 \tag{16}$$

(a typical example is the delta function).

Replacing $x = 2\theta z$ one can rewrite (13), for $\gamma = 0$, as the following

$$\frac{d^2F}{dz^2} + \frac{dF}{dz} = -\frac{\theta}{\theta_0} S\left[\frac{\theta}{\theta_0} z - \ln\frac{1}{\varepsilon} - y_1\right].$$

Recalling that in the time period under consideration, the macroscopic parameters have only minor changes and by neglecting them $N \simeq N_0$, $\theta \simeq \theta_0$, we have $F'' + F' = -S(y - y_1)$, where this equation is now considered for $-\infty < y < \infty$. Recognizing, as previously, $F(y) \to 0$ as $y \to \infty$, and making use of the sewing condition as $y \to -\infty$ with the Maxwellian distribution (14), we finally obtain

$$F(x) = Ce^{-x/2\theta} + \frac{1}{N}\int_{-\infty}^{x} dz\, e^{-(x-z)/2\theta} \int_z^\infty du\, S(u).$$

If, in particular, the source is a monokinetic distributed function $S(x) = I_+\delta(x - x_+)$, then for the Coulomb potential, $\gamma = 0$, the solution reads as

$$F(x) = C\exp\left[-\frac{x}{2\theta}\right] + \frac{I_+}{N}\left\{\eta[x_+ - x] + \eta[x - x_+]\exp\left[-\frac{x - x_+}{2\theta}\right]\right\}, \tag{17}$$

https://doi.org/10.1017/S0022377805003697 Published online by Cambridge University Press

where $\eta[y]$ is a unit function equal to 1 if $x > 0$ and equal to 0 if $x < 0$. In the general case of $\gamma > 0$, we have

$$F(x) = Ce^{-x/2\theta} + \frac{1}{N}\int_x^\infty S(z)\,dz \int_{-\infty}^x e^{-(x-z)/2\theta} z^{-\gamma}\,dz$$
$$+ \frac{1}{N}\int_{-\infty}^x S(z) \int_{-\infty}^z u^{-\gamma} e^{-(x-u)/2\theta}\,du\,dz. \tag{18}$$

The integrals in (18) for the dipole interaction $\gamma = 1$ can be expressed through the integral exponential function $\mathrm{Ei}(x)$ (or $\mathrm{li}(e^x)$) and for the Maxwell molecules $\gamma = \frac{3}{2}$ they are reduced to the Dawson's integral.

Thus, we obtain the intermediate asymptotic that is exact under the conditions $t \to \infty$, $\varepsilon \to 0$, $x \to \infty$, such that

$$\triangle t = \varepsilon \cdot \ln\frac{1}{\varepsilon} \cdot t \quad \text{is finite}, \quad y_1 = \left(\frac{x}{2\theta_0} - \ln\frac{1}{\varepsilon}\right) \quad \text{is finite}. \tag{19}$$

The range of the interval $\triangle t$ can be estimated from the expressions (8), (12), (16). Within the time interval under consideration $\triangle t$ (19), which is rather large, the density and the energy practically do not undergo noticeable changes and sources are regarded as still located in a tail distribution region. However, at the same time the new quasi steady-state distribution function is established.

Note, that all arguments are valid for sinks (negative sign of sources), as well as for a number of sources.

3. The mechanism of particle distribution formation in the presence of external pumping

We note several items concerning the subsequent numerical treatment. The problem examined here through numerical simulation faces the principal obstacle of being concluded in the nonlinearity of the equation, when in the absence of sources (sinks), two conservation laws (density and energy) are valid for one isotropic nonlinear LFP operator. In a discrete case, satisfying both these laws simultaneously is very important; otherwise, as a result of dissipative properties of usual difference schemes, simulation results might be unreliable and substantially distorted by the fictitious sources and sinks. Numerical simulation illustrates and confirms the results obtained in the preceding section. The comparison of the numerical calculations with the analytical asymptotic results in turn proves the high accuracy of the exploited difference algorithm that properly takes the nonlinearity of the LFP equation into account. Examples that display common features of the process under investigation and for the parameters that are rather far from those considered analytically are given. Considering the experimental situation on irradiation of a thin GaAs film by a fast ion beam [8], we provide a comparison of the results obtained in the experiment with those obtained by numerical simulation. Then we conduct the qualitative illustrative comparison of the NE electron distributions obtained numerically with those adapted from [7].

For numerical modelling we deal with the dimensionless nonlinear LFP operator (5) using the scaled variables introduced in the last section. The symmetrical

https://doi.org/10.1017/S0022377805003697 Published online by Cambridge University Press

kernel $Q(v,w)$ for the power law interaction potentials can be written as follows [9]:

$$Q(v,w)=\frac{a(v,w)(v+w)^{\eta+4}+b(v,w)|v-w|^{\eta+4}}{(\eta+2)(\eta+4)(\eta+6)}$$

with

$$a(v,w)=[(\eta{+}4)vw{-}(v^2{+}w^2)],\quad b(v,w)=[(\eta{+}4)vw{+}(v^2{+}w^2)],\quad \eta=(\beta{-}4)/\beta.$$

Negative values of η correspond to the soft interaction potentials with $1\leqslant\beta<4$. For charged particles with $\beta=1$ ($\eta=-3$) we have $Q(v,w)=(2/3)w^3,\ w\leqslant v$ and $Q(v,w)=(2/3)v^3,\ w\geqslant v$.

To compose the difference scheme we replace the infinite velocity interval $[0,\infty)$ by the finite segment $[0,v_{\max}]$, which is chosen so as to take into account the high-energy particles, and let the boundary condition for the distribution function be $f(v_{\max},t)=0$. The source and sink action are included in (6) mainly in the form of a δ-function: $S_\pm\sim I_\pm\cdot\delta(v-v_\pm)/v^2$. If the intensity $I_+=I_-\cdot {v_-}^2/{v_+}^2$, then the energy that comes from external sources equals zero and we deal with an analogue to a particle flux. If intensities are equal to each other, $I_+=I_-$, then the particle density is constant over the process. In addition, we consider exponentially distributed sources and sinks $S_\pm\sim I_\pm\exp[-b(v-v_\pm)^2]$ to examine whether the NE distribution depends on the shape of the source (sink) function. The delta function $\delta(v-v_1)$ is approximated by the discrete function that differs from zero at a single velocity point $v=v_1$.

We take an initial function either a function similar to the Maxwellian distribution

$$f^0(v)=\frac{4}{\sqrt{\pi}}\left(\frac{3}{2}\right)^{3/2}\exp\left[-\frac{3}{2}v^2\right],\quad N_0=1,\quad \theta_0=\frac{1}{3},$$

or a δ-function type distribution. In the absence of external sources, $I_\pm=0$, the latter case is a Cauchy initial problem which models the relaxation of the initial beam-like distribution to the equilibrium function [11].

To make contact with the asymptotic treatment of the last section, we consider the time evolution of the initial distribution function for $\beta_{1,2,3}=1,2,4$ under the source with relatively small intensities when sinks are absent. The formation of the NE distribution can be divided into three parts. During the first short stage, the system 'remembers' the initial conditions and the initial distribution function form. This time period of the relaxation is of the order of $t\sim 1$ and is approximately equal for different values of β. During the second stage, the formation of the NE distribution bulk takes place. The duration of this stage depends on the placement of the source position v_+, but it is independent of the source function form and of its intensity. After the NE distribution part has formed, it takes a flattening shape or a very gradually decreasing function of velocity between the source and the cold particle region. The establishment of the steady-state distribution is accomplished with the distribution function tails' formation. The length of the third stage is sufficiently dependent on different β. In Fig. 1, the NE steady-state distribution function is shown in the logarithmic scale versus the energy (squared velocity). The computations were carried out for the source position $v_+=6$ and for the intensity $I_+=10^{-6}$. It may be observed clearly that the form of the steady-state distribution is in good agreement with the analytical solution. The NE distribution manifests a dramatic increase within the velocity interval between the source and the bulk particle distribution. The time evolution of the chief part of the NE distribution is

https://doi.org/10.1017/S0022377805003697 Published online by Cambridge University Press

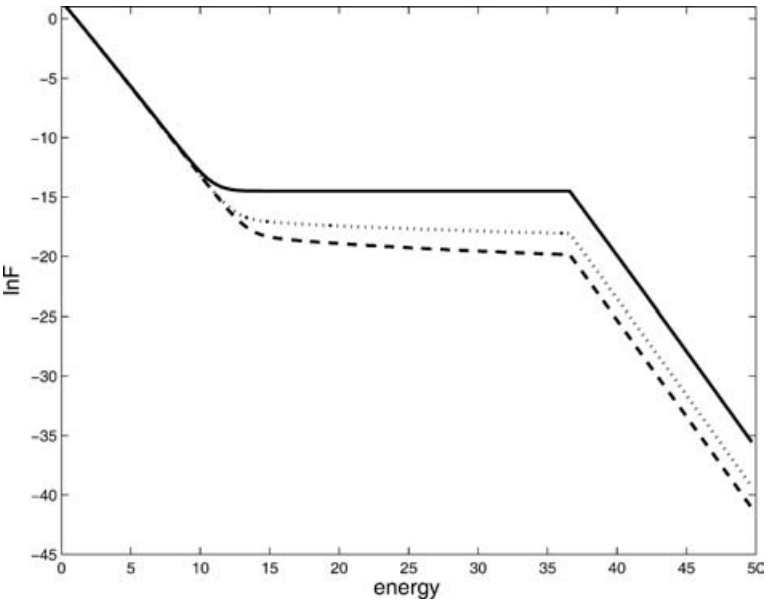


Figure 1. Logarithm of the steady-state NE distribution function versus squared velocity (arbitrary units). The computations were carried out for the source located at $v_+ = 6$, for the intensity of $I_+ = 10^{-6}$ and for $\beta = 1, 2, 4$ (full, dotted and dashed curves, respectively). Sinks are absent.

terminated at $t \simeq 50$ for $\beta = 1$, at $t \simeq 2$ for $\beta = 2$, and $t \simeq 1$ for $\beta = 4$. To represent the formation of the distribution function in the far tail region we use the deviation φ from the Maxwellian distribution: $f = f_{\mathrm{MW}}(1+\varphi)$ and depict the process in Fig. 2 for $\beta = 1$ and in Fig. 3 for $\beta = 4$. As can be seen, the process of a tail formation comes after the beam relaxation pattern. For Coulomb interaction, the spreading of φ with time into the high-velocity region has the character of a propagating wave with a stable front. For dipole interaction, $\beta = 2$, the spreading still preserves the wave-like character with a slightly broadening front. For the Maxwell molecules with stiffer interaction potential, $\beta = 4$, the formation of the main NE distribution part occurs simultaneously with the tail distribution formation.

Figure 4 demonstrates the steady-state distribution being formed under the action of the source and sink that are placed at $v_+ = 6$ and $v_- = 3.5$, correspondingly, and distributed as the Gaussian function with $b = 10$. As can be seen the source spread shape slightly manifests itself in the form of a solution in the vicinity of v_+, but changes none of the general functional characteristics. To expose the very gradual declination of the distribution more evidently, the bottom part of Fig. 4 shows the presented solution with its NE part more pronounced at the point v_-.

Figure 5 gives an example of the simulation run for $\beta = 2$ and $I_+ = 10^{-5}$, $I_+ = 10^{-8}$ and $v_+ = -5$, $v_+ = 8$. Sinks are absent. One can see the heights of plateaus are proportional to the magnitude of intensity that coincides with the analytical predictions. For the intensity of $I_+ = 10^{-8}$, the overheated population of the particle spectrum is stretched out to the region $v \simeq 4$ and for the intensity $I_+ = 10^{-5}$, it extends to $v \simeq 3$, which is relatively close to the distribution core. Figure 5 displays that declination of the distribution functions in the tail region $v \geqslant v_+$ is the same for different intensities; that is, the tails have the same temperature. Obviously, the

https://doi.org/10.1017/S0022377805003697 Published online by Cambridge University Press

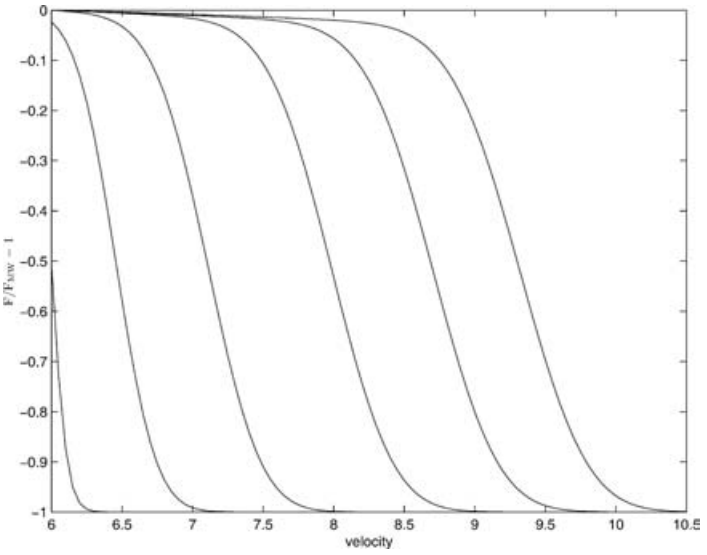


Figure 2. Distribution function formation in the tail velocity region presented by the deviation $\phi = f/f_{\mathrm{MW}} - 1$ for $\beta = 1$, $v_+ = 6$, $I_+ = 10^{-6}$ and at the time moments $t = 1, 10, 25, 50, 100, 150$.

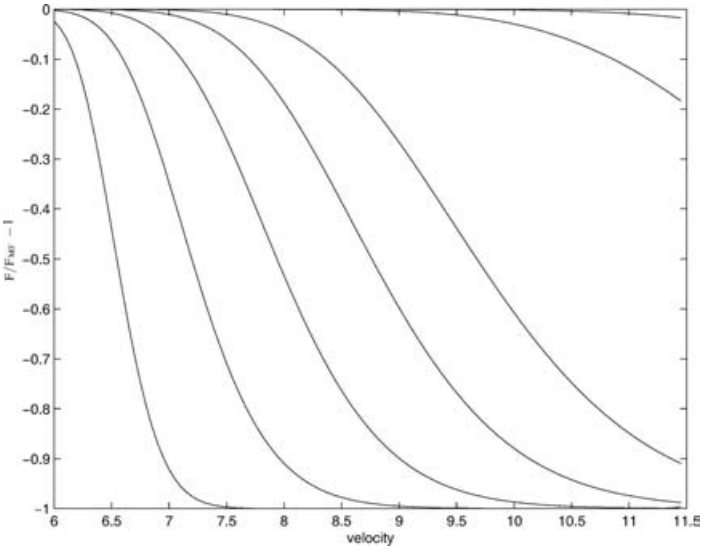


Figure 3. The distribution function formation in the tail region for $\beta = 4$ and at the time moments $t = 0.05, 0.1, 0.15, 0.2, 0.25, 0.4, 0.5$.

pronounced plateau form (for $\beta = 1$) of the steady-state distribution depends on the interplay between the source intensity and the collision action. In the case of small intensities, the NE function becomes less flattened and has a more evident slope.

The functional dependence of the steady-state NE electron distribution is not sensitive either to the extent to which the source and sink are located in momentum space or to the length of the inertial interval, i.e. the interval between the source

https://doi.org/10.1017/S0022377805003697 Published online by Cambridge University Press

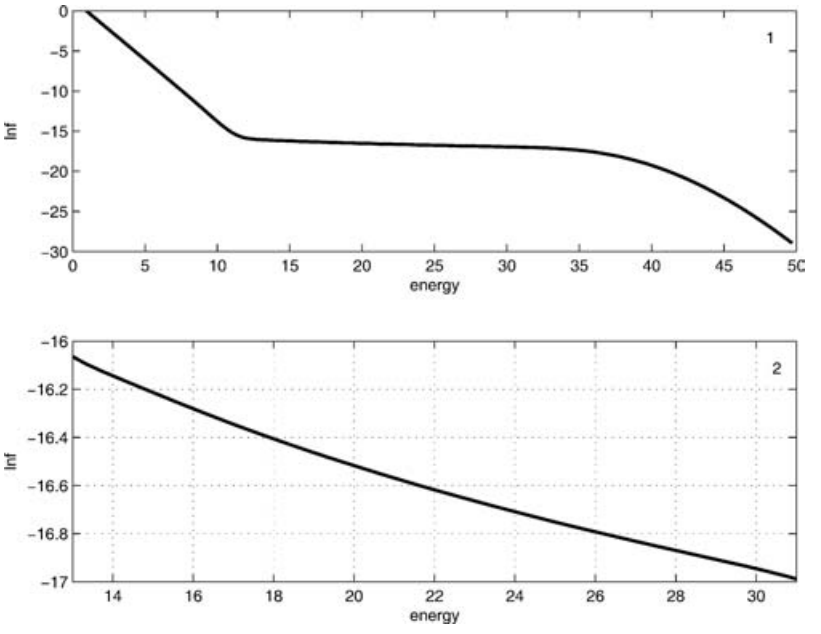


Figure 4. Non-equilibrium distribution function for $\beta = 2$ for the source and sink function distributed as a function (15) for $I_+ = I_- = 10^{-6}$, the sink location is at $v_- = 3.5$ and the source position is at $v_+ = 6$.

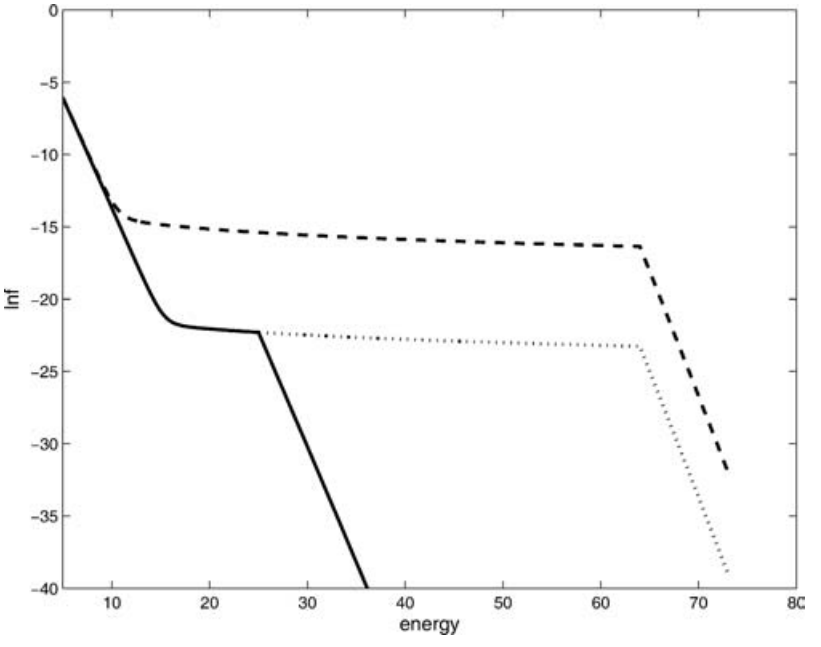


Figure 5. Steady-state distribution function for $\beta = 2$ versus squared velocity for the source located at $v_+ = 8$ with intensity $I_+ = 10^{-5}$ (dashed curve), for the intensity $I_+ = 10^{-8}$ and $v_+ = 8$ (dotted curve), and for the source located at $v_+ = 5$ with intensity $I_+ = 10^{-8}$ (full curve).

https://doi.org/10.1017/S0022377805003697 Published online by Cambridge University Press

and the sink. From our consideration it follows that even the relative smallness of sources may imply a drastic deviation of the steady-state distribution function from the equilibrium distribution. The remarkable result is that within a very long time interval (19) while neither density nor energy change much, the new quasi-steady-state distribution function is established. This interval can last for hundreds of collision times and NE distribution may differ from the equilibrium function by tens of orders in magnitude. Numerical results also show that the analytical asymptotic estimations obtained for the linear case are fit for a wider class of parameters.

To analyze the results of the experiment on the irradiation of a thin semiconductor film of GaAs by a beam of proton ions [8], it is worth noting that the electron distribution function formation happens independently on every ion track even for high ion beam intensities corresponding to the inertial fusion parameters. Moreover, the formation of the electron distribution function occurs by means of the electron–electron collisions rather than by the electron–phonon collisions [3]. It is well known that a fast ion, the velocity of which is commensurable or exceeds the speed of an electron in the Bohr's orbit, interacts mainly with binding and free electrons. In doing so, the ion produces atom excitation and ionization by direct electron impact, as well as, from the excitation of wake plasma waves by ion collisions. We evaluate the parameters corresponding to the conditions of the experiment [8].

Note that the free path of ion H^+ with energy 1.25 MeV in GaAs is $l = 3 \times 10^{-6}$ m, the ion speed corresponding to an energy of 1 MeV is equal to $v_{\mathrm{Ht}} = 7.5 \times 10^6$ m s^{-1}. From this, we compute the time period in which the proton loses the main part of its energy $t_{\mathrm{tr}} = 4 \times 10^{-13}$ s. For a given test specimen of gallium arsenide, the electron density is $n_{\mathrm{e}} = 5 \times 10^{24}$ m^{-3} and the characteristic velocity in such a semiconductor plasma is $v_{\mathrm{th}} = 6 \times 10^5$ m s^{-1}. Then the corresponding characteristic electron–electron relaxation time is of the order of $t_{\mathrm{ee}} = 3 \times 10^{-14}$ s. We see that a sufficient quantity of collisions takes place in the time of the electron free path and under this condition the NE distribution function is developed due to the flux presence in the velocity space. Let us estimate the intensity of the sources arising due to the electron ionization by the direct electron impact and owing to the plasma wave excitation. Along the full free path the ion creates, about 10^4 electrons, in this case the characteristic volume, where ionization will be produced equals 3×10^{-21} m^3. The density of new electrons being produced in a time unit is about $I_+ \approx 3.3 \times 10^{37}$ m^{-3} s^{-1}. In the collision integral the normalization units are n_{e} and t_{ee}, then the normalized intensity is about 0.01–0.1 and the normalized time of the source action is of the order of 10. Two different source positions in the velocity space have correlation with the plasmon ionization at the characteristic speed $v_{+,1} \approx 3.5$ and with the ionization by the electron impact at $v_{+,2} \approx 7$. In the considering experimental situation, the principal losses are the ion–electron emission from the film surface. Electrons with energy higher than the outputting work and the retarding potential may be adrift and emerge from the sample within time τ_{ex} for the width of the emitting layer $d_{\mathrm{em}} = v_{\mathrm{th}}\tau_{\mathrm{ee}}$ which exceeds the electron free path length λ in semiconductor. The sink is assumed to be zero down to the energy $\mathscr{E} = E_{\mathrm{F}} + A \approx 5.65$ eV and distributed over the momentum space as

$$S_- = \frac{\tau_{\mathrm{ee}}}{\tau_{\mathrm{ex}}} f\left(\frac{v}{v_{\mathrm{th}}}\right) = \frac{\lambda v \tau_{\mathrm{ee}}}{{d_{\mathrm{em}}}^2} f\left(\frac{v}{v_{\mathrm{th}}}\right) \approx 0.05 \frac{v}{v_{\mathrm{th}}} f\left(\frac{v}{v_{\mathrm{th}}}\right).$$

We consider the source intensities' range 0.01–0.1, the variation of which can be connected both with the differing power of the bombarding ion beams and with

https://doi.org/10.1017/S0022377805003697 Published online by Cambridge University Press

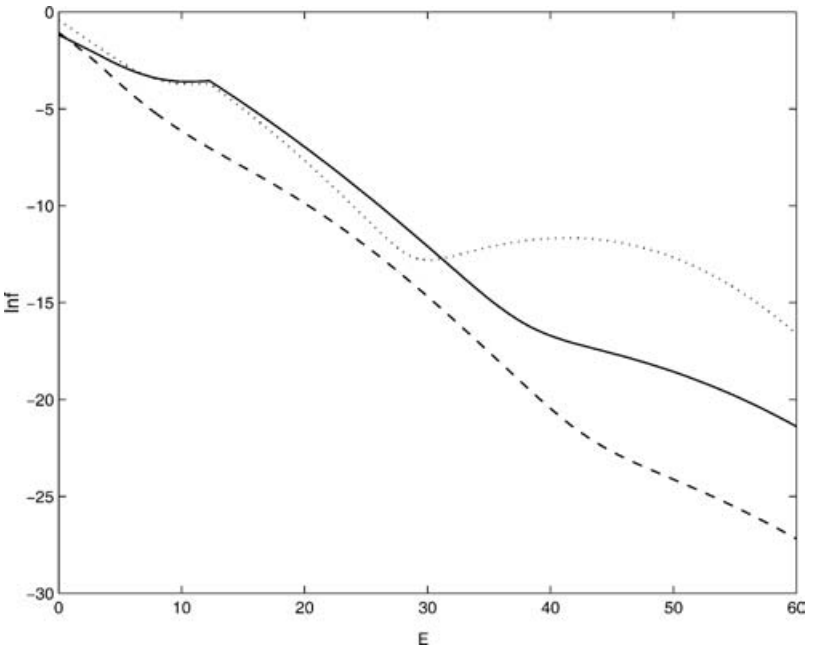


Figure 6. The distribution function $f(v)$ evolution versus squared velocity (energy): the dotted curve, $t = 15$; the solid curve, $t = 20$; the dashed curve, $t = 30$. The source with intensity $I_{+,1} = 0.1$ at $v_{+,1} = 3.5$ is turned off since $t = 20$; the source with intensity $I_{+,2} = 0.075$ at $v_{+,2} = 7$ is turned off since $t = 2$. The losses with intensity $I_{-} = 0.075$ act in a region of $v > 2$.

the difference in electron density between samples. Figure 6 shows the distribution function formation for the sources 1 and 2; they are turned off at $t = 20$. Losses act upto the time $t = 100$. The quasi stationary NE distribution is formed in a time of about 10–15 and has a character which is substantially distinguished from the power-like functional dependence obtained in [3]. The explanation can be attributed to the fact that sources and sinks being distributed over the velocity space do not provide the constant energy flux (and the concurrent zero density flux). In accordance with the above results, the NE function establishing is independent of the intensity value.

Let us compute the emission current dependence on the retarding potential U, which is needed to analyze the energetic spectrum of the electron emission in the experiment

$$J = \text{constant} \cdot \int_{E_F+U+A}^{\infty} dE\, f(E)E,$$

where A is an electron output work. For the experimental conditions have been studying, the electron energetic spectrum of ion–electron emission would be quasi-stationary for the ion beam currents exceeded 1–10 mA. In this case, the emission current is certainly defined by the different ion tracks dispersed in a space, but the distribution function of emission electrons is practically quasi-stationary, which leads to the quasi-stationary emission current. From the comparison of variants, we see how the difference in the emission electron current dependence is strong for

https://doi.org/10.1017/S0022377805003697 Published online by Cambridge University Press

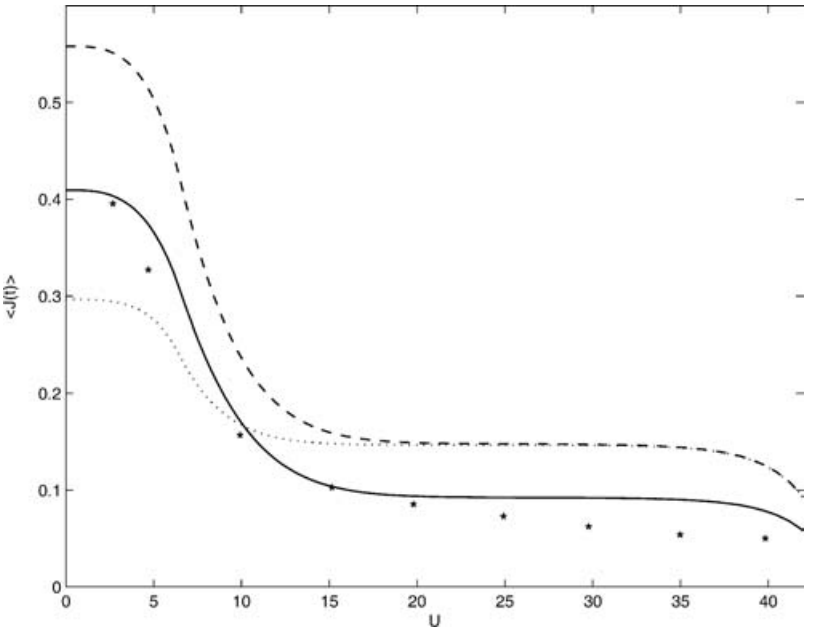


Figure 7. Current dependence versus the retarding potential: the dotted curve is for the current averaged over $t = 10$; dashed curve, $t = 20$; the solid curve, $t = 100$, and asterisks denote the experimental results [8].

the different endurance of the source action. In the experimental conditions [8], the current of the ion beam does not exceed 10 μA. In this case, the emission current will fully reflect the non-stationary character of the sources. On each ion track, the distribution function has time enough to go through all stages of its formation. That is why the emission current dependence on the retarding potential observed in the experiment is a superposition of the currents existing in different time stages. Obviously, the electron energetic spectrum differs from that formed under the stationary source action. The emission current dependence on the retarding potential is depicted in Fig. 7. The comparison of the simulation and experimental results shows that taking into account the non-stationary source character may be the determining factor.

We make a comparison of the numerically obtained distribution functions with the electron energy distributions adapted from [7]. They correspond to the secondary electron emission induced by 1 keV electrons for polycrystalline Al, Mg. These materials are not semiconductors and then, strictly speaking, to describe them it is necessary to use Boltzmann's collision integral. However, as it is shown, for example in [8], there is some similarity between the spectra of electrons emitted from metals and semiconductors. The plasmon energy 10.5 eV and $\mathscr{E} \approx 4.64$ eV were taken for Mg, and for Al the plasmon energy is ≈ 15.5 eV and $\mathscr{E} \approx 5.25$ eV [17, 18]. Figure 8 shows the electron distribution functions for different time moments, data from [7] are inserted with asterisks. Despite the fact that certain arbitrariness remains in comparing data, the characteristic features of the distribution functions, as can be seen, are in a good qualitative agreement.

https://doi.org/10.1017/S0022377805003697 Published online by Cambridge University Press

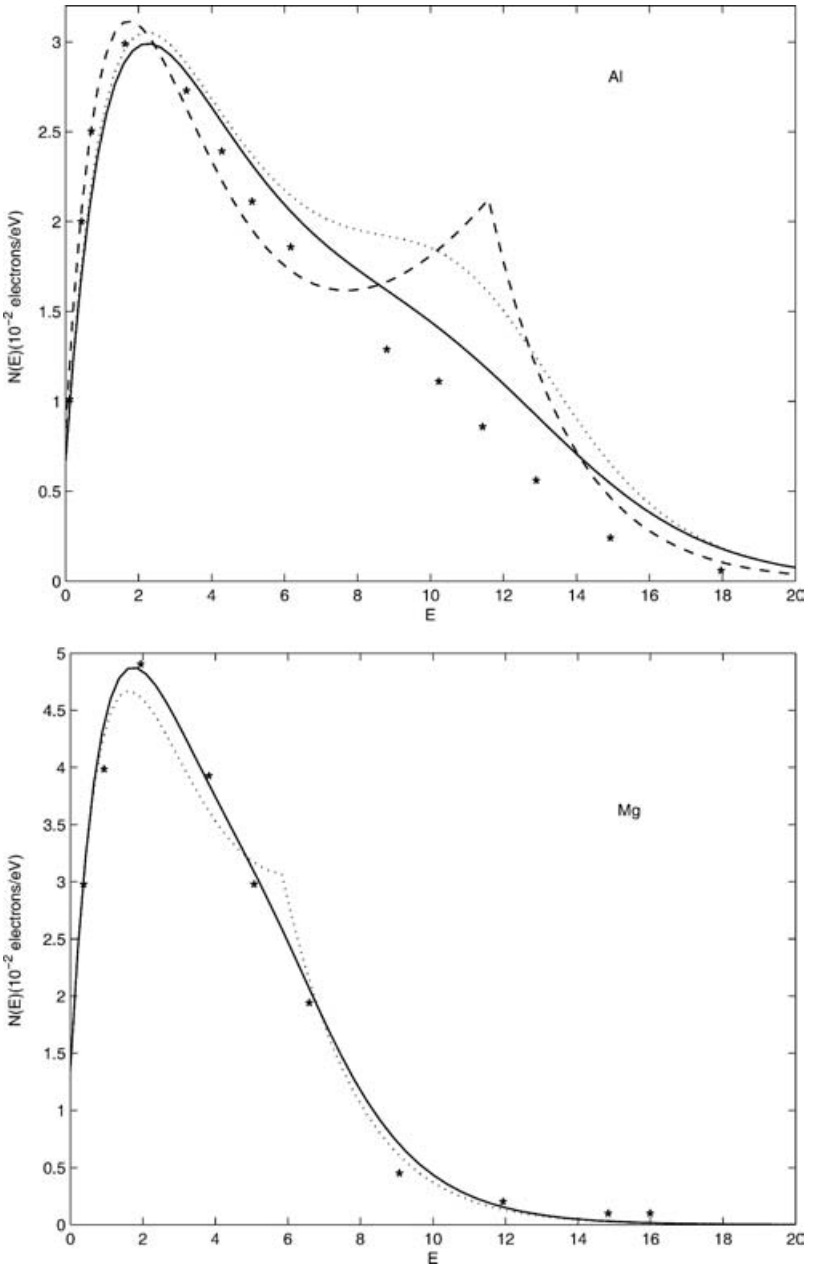


Figure 8. Electron energy distributions $N(E)$ for Al and Mg: the dashed curve, $t = 20$; the dotted curve, $t = 25$; the solid curve, $t = 30$; and asterisks denote data adapted from [7].

4. Conclusions

The nonlinear Landau–Fokker–Planck kinetic equation for the power-like potentials $U \sim \alpha/r^{\beta}, 1 \leqslant \beta < 4$, is considered in the presence of energy (particle) sources (sinks). The rigorous asymptotic estimation and the applicability conditions for the asymptotic steady-state solution are given. The detailed analysis of the time

https://doi.org/10.1017/S0022377805003697 Published online by Cambridge University Press

evolution and distribution function structure is carried out numerically. Particular emphasis is placed on the accuracy and high efficiency and reliability of the employed finite different schemes. As can be expected, the very gradually decreasing function in the inertial interval is established.

From our consideration it follows that, even relative smallness of sources may imply a drastic deviation of the steady-state distribution function from the equilibrium. The NE distribution may differ from the equilibrium function by tens of orders in magnitude. The conduction characteristics of the medium are governed by the density of the current carriers, so that, in a semiconductor plasma with a NE electron distribution, this density is very high, in contrast to the case of an exponentially decreasing equilibrium distribution function. That is why, under the action of intense fluxes of electromagnetic radiation or fast particles, the emission and conduction properties of a semiconductor plasma can become anomalous. With these findings from the NE distribution functions the behavior of the semiconductor plasmas can be predicted and explained. Obtained results can serve as a test problem and can be incorporated in more complicated models that include similar physical effects. Results of simulation are consistent with asymptotic and experimental results. In particular, in experiments on irradiation of a thin GaAs film by a fast ion beam, the comparison shows that the taking into account the source non-stationarity may be the determining factor. The obtained results can be useful in connection with the development of high-power particle and energy sources and for the prediction of the semiconductor behavior under the action of particle fluxes or electromagnetic radiation.

Acknowledgements

Authors would like to thank Professor A. V Bobylev for valuable comments. IFP is grateful to Dr. O. Maj for his hospitality at the Physics Institute 'A. Volta' of Pavia University. This work is partially supported by the Cariplo Foundation, the Landau Network-Centro Volta.

References

[1] Kolmogorov, A. N. 1941 *Dokl. Akad. Nauk SSSR* **30**, 299.

[2] Zakharov, V. E. 1965 *Zh. Prikl. Mekh. Tekh. Fiz.* **4**, 35.

[3] Kats, A. V., Kontorovich, V. M., Moiseev, S. S. and Novikov, V. E. 1975 *JETP Lett.* **21**, 5.
Karas', V. I., Moiseev, S. S. and Novikov, V. E. 1975 *JETP Lett.* **21**, 525.
Karas', V. I. 1975 *JETP Lett.* **1**, 1020.

[4] Carlile, R. N. and Webster, S. J. 1988 *IEEE Transactions on Plasma Science* **16**, 17.

[5] Aseevskaya, A. S., Ivkin, E. B. and Kolomiets, B. G. 1976 *Sov. Tech. Phys. Lett.* **2**, 117.

[6] Balebanov, V. M., Karas', V. I., Karas', I. V., Kononenko, S. I., Moiseev, S. S., Muratov, V. I. and Naguchev, O. Yu. 1998 *Plasma Phys. Rep.* **24**, 732.

[7] Baragiola, R. A., Dukes, C. A. and Riccardi, P. 2001 Plasmon excitation in ion–solid interactions. *Nucl. Instrum. Meth.* B **182**, 73.

[8] Kononenko, S. I., Balebanov, V. M., Zhurenko, V. P., Kalantar'yan, O. V., Karas', V. I., Kolesnik, V. T., Muratov, V. I., Novikov, V. E., Potapenko, I. F. and Sagdeev, R. Z. 2004 *Plasma Phys. Rep.* **30**, 687.

[9] Potapenko, I. F. and de Azevedo, C. A. 1999 *J. Comput. Appl. Math.* **103**, 115.

[10] Bobylev, A. V., Potapenko, I. F. and Chuyanov, V. A. 1980 *Zh. Vychisl. Mat. Mat. Fiz.* **20**, 993.

https://doi.org/10.1017/S0022377805003697 Published online by Cambridge University Press

[11] Potapenko, I. F., Bobylev, A. V., de Azevedo, C. A. and de Assis, A. S. 1997 *Phys. Rev.* E **56**, 7159.

[12] Grad, H. 1957 Principles of the kinetic theory of gases. *Handbuch der Physik 12*. Berlin: Springer.

[13] Landau, L. D. and Lifshits, E. M. 1975 *Mechanics*. Oxford: Pergamon.

[14] Landau, L. D. 1937 *Zh. Eks. Teor. Phys.* **7**, 203.

[15] Rosenbluth, M. N., McDonald, M. and Judd, D. 1957 *Phys. Rev.* **107**, 1.

[16] Bobylev, A. V. 1988 *Mathematical Physics Reviews* (eds. S. P. Novikov and Ya. G. Sinai). New York: Harwood Academic **7**, 111.

[17] Platzmann, P. M. and Wolf, P. A. 1973 *Waves and Interactions in Solid State Plasmas*. New York: Academic Press.

[18] Kittel, C. 1963 *Quantum Theory of Solids*. New York: Wiley.

https://doi.org/10.1017/S0022377805003697 Published online by Cambridge University Press